

Terahertz nanoresonators: Giant field enhancement and ultrabroadband performance

H. R. Park,¹ Y. M. Park,¹ H. S. Kim,¹ J. S. Kyoung,¹ M. A. Seo,¹ D. J. Park,² Y. H. Ahn,² K. J. Ahn,¹ and D. S. Kim^{1,a)}

¹Department of Physics and Astronomy, Center for Subwavelength Optics, Seoul National University, Seoul 151-747, Republic of Korea

²Division of Energy Systems Research, Ajou University, Suwon 433-749, Republic of Korea

(Received 20 January 2010; accepted 2 March 2010; published online 24 March 2010)

Transmission of terahertz (THz) electromagnetic waves through a series of nanoresonator arrays punctured in a thin metallic film is investigated. Over 30% of normalized transmitted amplitude is observed with only 0.18% of aperture-coverage, implying an electric field enhancement of 170. Increasing the coverage to 0.6% results in a 90% normalized amplitude, with a broader line width. Inspired by log-periodic antenna, we put ten nanoresonators with four different lengths per unit cell, succeeding in an ultrabroadband THz filter with one decade width between 0.2 and 2.0 THz. © 2010 American Institute of Physics. [doi:10.1063/1.3368690]

Shape resonance phenomena in metallic rectangular hole structures in microwave, terahertz (THz), and optical regions have long been a topic of interest both from fundamental aspect as well as for their application potentials.¹⁻⁹ Resonance behavior has been investigated at feature sizes smaller than the wavelength but far greater than the skin-depth. In this region, it has been shown, theoretically and experimentally, that the field enhancement inside holes increases as the width decreases.^{10,11} Recently, it was reported that one-dimensional nanoslits enhances electric field in the THz frequency range by orders of magnitudes with resonance-less $1/f$ frequency dependence.¹² One prominent question is then whether hundreds of micron long rectangular holes with nanosized widths, called THz nanoresonators, also allow a large enhancement of the electric field particularly at resonance, thereby resulting in much enhanced transmission.

In this paper, we show that nanorectangular apertures with width $w=200$ nm and length $l=100$ μm funnels THz electromagnetic waves through, accompanied by a large field enhancement unavailable for micron-scale aperture widths.^{11,13} With the aperture size several times larger than the skin-depth, theory based on the perfect conductor approximation still gives good agreement. With close-packing of different-length antennas per unit cell, namely ten nanoslot antennas with four different l , we achieve essentially flat, ultrabroadband transmission spectrum spanning over one decade.

We first consider an array of rectangular holes in a metallic film with 100 nm thickness on a dielectric substrate of 450 μm thick undoped silicon. These THz nanoresonators in dimensions of 100 $\mu\text{m} \times 200$ nm ($l \times w$), acting as slot antennas, enhance transmittance at the resonance frequency of 0.6 THz, which is $\sim c/(2n_{\text{eff}}l)$ where n_{eff} is the effective refractive index of the substrate¹⁴ [Fig. 1(a)]. We pattern these nanoresonators by electron beam lithography using a negative photoresist and the single-layer lift-off process [Fig. 1(b)]. This fabrication method allows access to an extreme ratio rectangular hole with a submicron sized width preserving a hundred micron-sized length.

To obtain a normalized transmitted amplitude through THz nanoresonators, we perform THz time domain spectroscopy^{15,16} in a frequency range from 0.2 to 2.0 THz with a single-cycle THz source generated from a 2 kV/cm biased semi-insulating GaAs emitter illuminated by a femto-second Ti:sapphire laser pulse train of a center-wavelength 780 nm, a 76 MHz repetition rate and a 130 fs pulse width [Fig. 1(c)]. By Fourier-transforming the time domain data, transmitted amplitude spectra for our sample, $E_{\text{sample}}(\omega)$, are obtained with phase information intact. For normalization of the measured spectrum, we use a reference signal, $E_{\text{ref}}(\omega)$, for the bare substrate after passing through a 1 mm by 1 mm metal aperture. We define the normalized (transmitted) amplitude $[T(\omega)]$ against the aperture field as the ratio between two measured amplitudes,

$$T(\omega) = |E_{\text{sample}}(\omega)/E_{\text{ref}}(\omega)|.$$

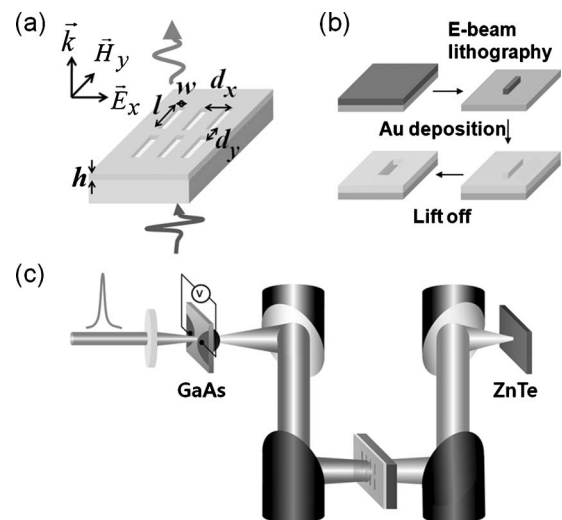


FIG. 1. (a) Schematic of an array of rectangular holes with the length l , the width w , d_x , and d_y the periods in x and y directions, respectively, h the thickness of metal film deposited on Si substrate. (b) THz nanoresonators are fabricated by electron beam lithography using negative type of photoresist patterning. (c) Our experimental setup: THz time domain spectroscopy.

^{a)}Electronic mail: dsk@phya.snu.ac.kr.

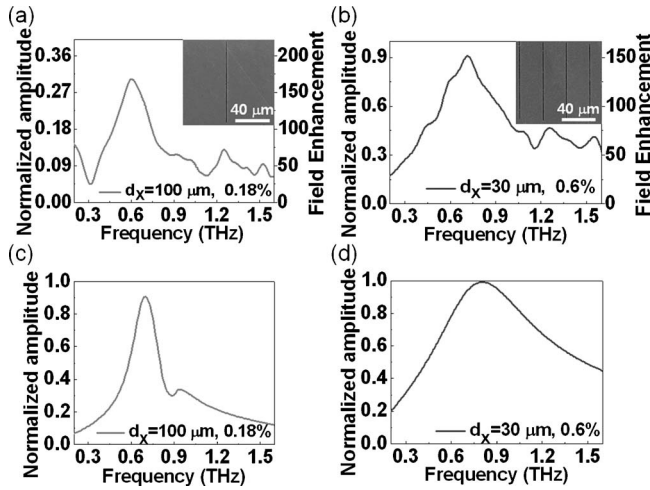


FIG. 2. (a) Normalized transmitted amplitude spectra measured through an array of nanoresonators with a length $l=100 \mu\text{m}$, a width $w=200 \text{ nm}$, and periods $d_x=100 \mu\text{m}$ and $d_y=110 \mu\text{m}$ (b) The same as (a) except $d_x=30 \mu\text{m}$. SEM images of the samples are shown in the insets. (c) A modal expansion based theoretical calculations with the period $d_x=100 \mu\text{m}$, and (d) $d_x=30 \mu\text{m}$.

THz nanoresonators with varying period d_x are investigated with polarization of the normally incident light along the width direction. Scanning electron microscope (SEM) images of these samples are shown in the insets of Figs. 2(a) and 2(b). Experimental results, shown in Figs. 2(a) and 2(b), are the normalized amplitude spectra for the period of $100 \mu\text{m}$ (coverage ratio of 0.18%) and $30 \mu\text{m}$ (coverage ratio of 0.6%), with fixed length $l=100 \mu\text{m}$ and width $w=200 \text{ nm}$. For the $30 \mu\text{m}$ period case, the normalized amplitude increases to over 90% at the resonance frequency despite the still tiny coverage of only 0.6%. This is in stark contrast with micropatterned samples, where it was found that to retain over 90% normalized amplitude, aperture coverage of over 12% was needed.⁹ While the field enhancement for the micropatterned sample was only 8,^{9,11} that for the 0.6% nanoresonator is over 150. This nanopattern superiority over micropattern results from the antenna cross section being relatively insensitive to the decreasing width. In addition, decreasing period pushes the Rayleigh minima out of the measurement range, again contributing to the enhanced transmission.¹⁷ Note also that the line width increases with higher coverage sample [Fig. 2(b)] relative to the low coverage sample [Fig. 2(a)]. We attribute this to higher scattering rate with larger number of apertures.

We compare our experiments with an analytical calculation based on modal expansion assuming perfect conductor and infinite array.¹⁸ With the single mode approximation counting only the half-wavelength mode for each rectangle, we obtain, for the zeroth order normalized transmitted amplitude (T_0) at normal incidence,

$$T_0 = \left(\frac{n+1}{2n} \right) \frac{2wl}{\pi d_x d_y} \frac{\frac{4i\mu}{k\pi}}{\left[W^2 + \left(\frac{2\mu}{k\pi} \right)^2 \right] \sin \mu h + 4 \frac{i\mu}{k\pi} W \cos \mu h},$$

where d_x, d_y are periods along the x and y directions, respectively, n the refractive index of substrate, k the wave vector of the incident light, h the thickness of metal, μ the waveguide vector, $\mu^2 = k^2 - (\pi/l)^2$, and finally W the self-

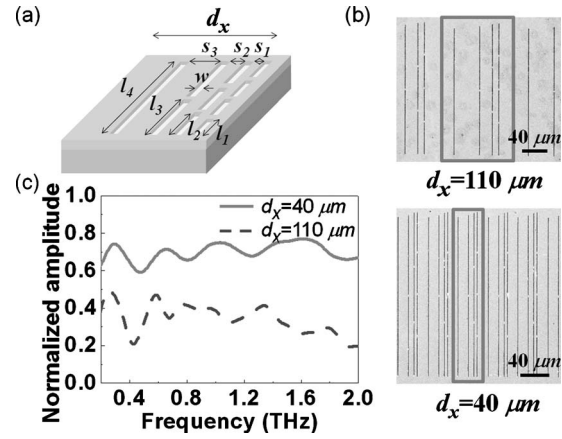


FIG. 3. (a) Schematic of log-periodic THz nanoresonators with four different lengths ($l_1=200 \mu\text{m}$, $l_2=100 \mu\text{m}$, $l_3=67 \mu\text{m}$, and $l_4=50 \mu\text{m}$), three different spacings (s_1, s_2 , and s_3), and the same width ($w=250 \text{ nm}$). (b) SEM images of the two samples with different periods: $d_x=110 \mu\text{m}$ ($s_1=40 \mu\text{m}$, $s_2=20 \mu\text{m}$, and $s_3=10 \mu\text{m}$) (top) and $d_x=40 \mu\text{m}$ ($s_1=15 \mu\text{m}$, $s_2=7 \mu\text{m}$, and $s_3=4 \mu\text{m}$) (bottom). Solid line boxes denote a unit cell in each structure. (c) Normalized amplitude spectra measured through the two samples with different periods of $110 \mu\text{m}$ (dashed line) and $40 \mu\text{m}$ (solid line) in the range between 0.2 and 2.0 THz.

illumination term describing coupling of the hole-eigenmodes with the incident wave.^{8,19,20}

Normalized amplitude curves obtained by the theoretical calculations, shown in Figs. 2(c) and 2(d), are in good qualitative agreement with experimental results, indicating that perfect conductor approximation still captures the essential physics including the increasing line width and blueshift of the peak position with decreasing period. However, for the $100 \mu\text{m}$ period case, the normalized amplitude value shows noticeable disagreement between the experimental result and theoretical model, most likely due to the small number of nanoresonators in each direction: only nine.^{21,22} For certain applications, ultrabroadband performance is needed while single resonance per unit cell may not give enough bandwidth.^{8,23} Multiple antennas per unit cell with different lengths could, in principle, provide the bandwidth encompassing all fundamental resonances corresponding to each length.

We now present an elegant way to achieve the ultrabroadband performance using a multi-antennas-per-unit cell idea, in the broad range from 0.2 to 2.0 THz. The unit cell structure borrows the concept of log-periodic antennas introduced by DuHamel and Isbell.^{24,25} In our unit cell, ten THz nanoresonators with four different lengths are contained, as shown in Fig. 3(a). The design rule is that: $l_1=200 \mu\text{m}$, $l_2=l_1/2=100 \mu\text{m}$, $l_3=l_1/3=67 \mu\text{m}$, and $l_4=l_1/4=50 \mu\text{m}$, with all antennas having the same width of 250 nm. To maintain the same coverage for each antenna length, we have four antennas in column with $l_4=50 \mu\text{m}$, three antennas with $l_3=67 \mu\text{m}$, and two antennas with $l_2=100 \mu\text{m}$. The spacing between the adjacent two antennas is arranged such that $s_1=2s_2=4s_3$. We consider two structures with different periods: $d_x=110 \mu\text{m}$; $s_1=40 \mu\text{m}$ and $d_x=40 \mu\text{m}$; $s_1=15 \mu\text{m}$, with the unit cells denoted by solid lines in Fig. 3(b). In Fig. 3(c), the normalized amplitudes for the samples show ultrabroadband spectra of over three octaves spanning from 0.2 to 2.0 THz. In the case of the period $d_x=40 \mu\text{m}$, the period pushes the Rayleigh minima out of our spectral range of the four fundamental resonances (0.35, 0.7, 1.1, and 1.5 THz) for

each length of nanoresonator, resulting in about 70% of normalized amplitude over the whole spectral range. With the recent introduction of active THz metamaterials controlled by an external stimulus,^{7,26,27} log-periodic THz nanoresonators can provide further progress toward ultrabroadband active metamaterials.

To conclude this paper, we have experimentally demonstrated that an ultrabroadband performance with an average normalized amplitude of 70% can be realized through log-periodic THz nanoresonators with a striking aspect ratio of a rectangular hole, 400:1, and large field enhancement in the THz region. It should be noted that nanoresonators have the decisive advantage over microns wide structures in that the lateral distances between two adjacent resonators can be very small, to be less than 5 μm . This ability to close-packing many antennas within small area, still maintaining a small coverage, is crucial in achieving the broad spectrum and high transmittance without sacrificing large field enhancement. The relatively broad spectrum of a single resonance structure with a period less than the half resonant wavelength is well-explained by our theoretical calculation, which helps explain the one-decade wide transmittance spectra of our multiresonance structure. THz nanoresonators with large transmittance maintaining small coverage open a strong possibility of potential applications, such as broadband field enhancement and nonlinear devices, filters, detectors, and active switching devices.

This work was supported by the Korea Science and Engineering Foundation (KOSEF) (SRC, Grant No. R11-2008-095-01000-0) and the Korea Research Foundation (KRF) grant funded by the Korea government (MEST) (Grant No. 2009-0071309), KICOS (GRL, Grant No. K20815000003), Seoul Science Fellowship, and the Seoul R&BD Program (Program No. 10543).

¹C. C. Chen, *IEEE Trans. Microwave Theory Tech.* **18**, 627 (1970).

²R. Ulrich and M. Tacke, *Appl. Phys. Lett.* **22**, 251 (1973).

- ³F. Keilmann, *Int. J. Infrared Millim. Waves* **2**, 259 (1981).
- ⁴K. J. K. Koerkamp, S. Enoch, F. B. Segerink, N. F. van Hulst, and L. Kuipers, *Phys. Rev. Lett.* **92**, 183901 (2004).
- ⁵K. L. van der Molen, K. J. Klein Koerkamp, S. Enoch, F. B. Segerink, N. F. van Hulst, and L. Kuipers, *Phys. Rev. B* **72**, 045421 (2005).
- ⁶H. Cao and A. Nahata, *Opt. Express* **12**, 3664 (2004).
- ⁷H. T. Chen, W. J. Padilla, J. M. O. Zide, A. C. Gossard, A. J. Taylor, and R. D. Averitt, *Nature (London)* **444**, 597 (2006).
- ⁸J. W. Lee, M. A. Seo, D. J. Park, D. S. Kim, S. C. Jeoung, C. Lienau, Q. H. Park, and P. C. M. Planken, *Opt. Express* **14**, 1253 (2006).
- ⁹J. W. Lee, M. A. Seo, D. H. Kang, K. S. Khim, S. C. Jeoung, and D. S. Kim, *Phys. Rev. Lett.* **99**, 137401 (2007).
- ¹⁰F. J. García-Vidal, E. Moreno, J. A. Porto, and L. Martín-Moreno, *Phys. Rev. Lett.* **95**, 103901 (2005).
- ¹¹M. A. Seo, A. J. L. Adam, J. H. Kang, J. W. Lee, K. J. Ahn, Q. H. Park, P. C. M. Planken, and D. S. Kim, *Opt. Express* **16**, 20484 (2008).
- ¹²M. A. Seo, H. R. Park, S. M. Koo, D. J. Park, J. H. Kang, O. K. Suwal, S. S. Choi, P. C. M. Planken, G. S. Park, N. K. Park, Q. H. Park, and D. S. Kim, *Nat. Photonics* **3**, 152 (2009).
- ¹³F. Miyamaru and M. Hangyo, *Phys. Rev. B* **72**, 035429 (2005).
- ¹⁴J. H. Kang, J. H. Choe, D. S. Kim, and Q. H. Park, *Opt. Express* **17**, 15652 (2009).
- ¹⁵M. van Exter, C. Fattinger, and D. Grischkowsky, *Opt. Lett.* **14**, 1128 (1989).
- ¹⁶Q. Wu, M. Litz, and X. C. Zhang, *Appl. Phys. Lett.* **68**, 2924 (1996).
- ¹⁷J. W. Lee, M. A. Seo, D. S. Kim, S. C. Jeoung, C. Lienau, J. H. Kang, and Q. H. Park, *Appl. Phys. Lett.* **88**, 071114 (2006).
- ¹⁸H. Lochbihler and R. Depine, *Appl. Opt.* **32**, 3459 (1993).
- ¹⁹D. J. Park, S. B. Choi, Y. H. Ahn, Q. H. Park, and D. S. Kim, *J. Korean Phys. Soc.* **54**, 64 (2009).
- ²⁰D. J. Park, S. B. Choi, Y. H. Ahn, F. Rotermund, I. B. Sohn, C. Kang, M. S. Jeong, and D. S. Kim, *Opt. Express* **17**, 12493 (2009).
- ²¹A. I. Fernández-Domínguez, F. J. García-Vidal, and L. Martín-Moreno, *Phys. Rev. B* **76**, 235430 (2007).
- ²²D. Pacifici, H. J. Lezec, H. A. Atwater, and J. Weiner, *Phys. Rev. B* **77**, 115411 (2008).
- ²³J. G. Han, J. Q. Gu, X. C. Lu, M. X. He, Q. R. Xing, and W. L. Zhang, *Opt. Express* **17**, 16527 (2009).
- ²⁴R. H. DuHamel and D. E. Isbell, *IRE Natl. Conv. Rec.* **1**, 119 (1957).
- ²⁵C. A. Balanis, *Antenna Theory* (Wiley, New York, 2005).
- ²⁶H. T. Chen, W. J. Padilla, M. J. Cich, A. K. Azad, R. D. Averitt, and A. J. Taylor, *Nat. Photonics* **3**, 148 (2009).
- ²⁷T. Driscoll, H. T. Kim, B. G. Chae, B. J. Kim, Y. W. Lee, N. M. Jokerst, S. Palit, D. R. Smith, M. Di Ventra, and D. N. Basov, *Science* **325**, 1518 (2009).